International Journal of Computer Applications (0975 - 8887)
Volume 178 - No.14, May 2019

Free Vibration of Curved beams with Hierarchical Finite Element Method

Ramon Macedo Corrêa
Postgraduate Program in Civil Construction Engineering
PPGECC - UFPR

Marcos Arndt
Postgraduate Program in Civil Construction Engineering
PPGECC - UFPR

Roberto Dalledone Machado
Postgraduate Program in Civil Construction Engineering
PPGECC - UFPR

ABSTRACT

In this paper the use of Hierarchical Finite Element Method (HFEM) in free vibration of curved beams is explored. The traditional Finite Element Method has been applied in dynamic structural problems over the years, but when searching for higher vibration frequencies a great computational effort is necessary. In this context, two hierarchical finite element approaches are proposed in order to achieve more accurate results than simple FEM mesh refinement, called h refinement. The proposed HFEM uses the Lobatto and Bardell polynomials to p refinement. The results are compared with references found in literature.

General Terms

p refinement, Hierarchical refinement

Keywords

Hierarchical Finite Element Method, Finite Element Method, curved beams, free vibration

1. INTRODUCTION

Vibrations represent the dynamic behavior of a physical system that can be described by a mathematical model formulated by differential equations. The more complex the system, the more difficult it becomes to obtain the results of the differential equations [4]. In order to solve these differential equations an approximate method can be employed, such as the Finite Element Method (FEM).
The traditional FEM is widely used in the dynamic structures analysis, but presents high errors when searching for higher vibration frequencies. In order to improve FEM responses, two types of refinement may be employed: the h refinement and p refinement.
According to [3] major benefits of the hierarchical p-method are the retention of the stiffness coefficients as the order of interpolation is increased and the high rates of convergence possible without the need for mesh refinement. These benefits promote a decreasing in the computational effort involved.
The curved beam element has aroused interest in researchers for some reasons, among them the fact that it is a very efficient element and it provides insight into some aspects of shell element behavior [8].
A curved beam element with 2 nodes and some alternatives of shape functions using polynomials and trigonometric functions was proposed in [9]. The use of high order polynomials in order to describe the displacement fields was proposed by [5] for static problems and by [11] for free vibration analysis of curved beams.
An application of the FEM for free vibration analysis of arch with non-uniform cross-sectional area was presented by [13]. A comparison of some approximate methods such as the Ritz Method, the Rayleigh-Schmidt Method, the Galerkin Method and the Finite Element Method for free vibration of arches using the curved beam element was presented in [1].
Taking into account the effect of shear strain, an element with 4 degrees of freedom per node was proposed by [6] for free vibration of thick curved beams.
A two node element and a three node element for static analysis of thick curved beams were proposed by [10, 12].
The p-Fourier Element for free vibration analysis of thin and thick curved beams was presented in [8] and a four node C^0 finite element for free vibration of thick curved beam with constant and variable curvature was proposed by [16].
In this paper two elements with hierarchical p refinement are proposed for dynamic analysis of thin curved beams.

2. HIERARCHICAL FINITE ELEMENT METHOD

In hierarchical p refinement the approximate displacements fields response (u_{appro}) can be written as:

$$u_{appro} = \sum_{i=1}^{n} N_i \, a_i, \tag{1}$$

where N_i are the shape functions and a_i are the related degrees of freedom. Note that degrees of freedom are not necessarily related to nodes. The approximation is hierarchical if an increase from n to $n+1$ does not change the N_i shape functions ($i = 1$ to n). Two classes of shape functions are used for the displacement fields described later.

2.1 C^0 shape functions

The C^0 shape functions related to the nodal degrees of freedom are the linear Lagrange polynomials, which are described by the following expressions in the interval $[-1, 1]$:

$$N_1 = \frac{1-\xi}{2}, \quad (2)$$

$$N_2 = \frac{1+\xi}{2}. \quad (3)$$

When these shape functions are used, the nodal degree of freedom is the value of the function in the node (u_i).
The C^0 hierarchical p refinement is formulated using the Lobatto polynomials [14], obtained by the following expressions, in the interval $[-1, 1]$:

$$l_k(x) = \frac{1}{||L_{k-1}||_2} \int_{-1}^{x} L_{k-1}(\xi)\, d\xi \quad (4)$$

$$||L_{k-1}||_2 = \int_{-1}^{1} L_{k-1}^2(x)\, dx = \sqrt{\frac{2}{2k-1}} \text{ and } k \geq 3 \quad (5)$$

where L_k are:

$$\begin{aligned} L_0(x) &= 1; \\ L_1(x) &= x; \\ L_k(x) &= \frac{2k-1}{k}\, x\, L_{k-1}(x) - \frac{k-1}{k}\, L_{k-2} \end{aligned} \quad (6)$$

2.2 C¹ shape functions

The C^1 shape functions related to the nodal degrees of freedom are the cubic Hermite polynomials, which are described by the following expressions in the interval $[-1, 1]$:

$$N_1 = \frac{1}{2} - \frac{3}{4}\xi + \frac{1}{4}\xi^3, \quad (7)$$

$$N_2 = \frac{L_e}{8}(1 - \xi - \xi^2 + \xi^3), \quad (8)$$

$$N_3 = \frac{1}{2} + \frac{3}{4}\xi - \frac{1}{4}\xi^3, \quad (9)$$

$$N_4 = \frac{L_e}{8}(-1 - \xi + \xi^2 + \xi^3), \quad (10)$$

where L_e is the element length.
When these shape functions are used, the nodal degrees of freedom are the value of the function and the derivative of order 1 in the node (u_i and du_i/dx).
The C^1 hierarchical p refinement is formulated using the Bardell polynomials [2], obtained by the following expressions, in the interval $[-1, 1]$:

$$f_r(\xi) = \sum_{n=0}^{r/2} \frac{(-1)^n (2r-2n-7)!!}{2^n n! (r-2n-1)!} \xi^{r-2n-1}, \quad (11)$$

where $r!! = r\,(r-2)\cdots(2 \text{ or } 1)$, $0!! = (-1)!! = 1$, $r/2$ denotes its own integer part, and $r \geq 5$.

3. CURVED BEAM ELEMENT

In the thin curved beam element the extensional strain (ϵ), the rotation (ϕ) and the change of curvature (χ) are described in terms of the displacements and their derivatives according to classical thin shell theory, as shown in the following expressions [5, 11, 8, 7]:

$$\epsilon = \frac{du}{ds} + \frac{w}{R}, \quad (12)$$

$$\phi = \frac{u}{R} - \frac{dw}{ds}, \quad (13)$$

$$\chi = \frac{1}{R}\frac{du}{ds} - \frac{d^2 w}{ds^2}, \quad (14)$$

where R is the radius of the curved beam, u and w are the tangential and normal components of the displacement at s, respectively, and s is the curvilinear coordinate, as represented in Figure 1.

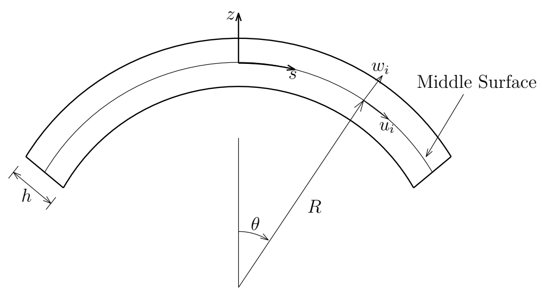

Fig. 1. Curved beam geometry.

The strain energy (U) and kinetic energy (T) expressions are written as:

$$U = \frac{1}{2}\int_0^{L_e} (E\,A\,\varepsilon^2 + E\,I\,\chi^2)\, ds, \quad (15)$$

$$T = \frac{1}{2}\int_0^{L_e} \rho\, A\,(\dot{u}^2 + \dot{w}^2)\, ds, \quad (16)$$

where E is the Young's modulus, A is the cross-sectional area, I is the moment of inertia and ρ is the material density. The displacements fields can be written as:

$$u = \sum P_i\, u_i \text{ and } w = \sum Q_i\, w_i, \quad (17)$$

where P_i and Q_i are the shape functions related to u and w, respectively, and u_i and w_i are the degrees of freedom also related to u and w, respectively.
Let $\{q\}$ be a vector containing the degrees of freedom related to u and w in the form:

$$\{q\} = \begin{Bmatrix} u_1 \\ \vdots \\ u_n \\ w_1 \\ \vdots \\ w_n \end{Bmatrix} \quad (18)$$

and let $\{N_P\}$ be a vector formed by the shape functions P_i and $\{N_Q\}$ a vector formed by the shape functions Q_i:

$$\{N_P\} = \begin{Bmatrix} P_1 \\ P_2 \\ \vdots \\ P_n \end{Bmatrix} \text{ and } \{N_Q\} = \begin{Bmatrix} Q_1 \\ Q_2 \\ \vdots \\ Q_n \end{Bmatrix} \quad (19)$$

and still

$$\overline{\{N_P\}} = \begin{Bmatrix} N_P \\ 0 \\ \vdots \\ 0 \end{Bmatrix} \text{ e } \overline{\{N_Q\}} = \begin{Bmatrix} 0 \\ \vdots \\ 0 \\ N_Q \end{Bmatrix} \quad (20)$$

so that $\overline{\{N_P\}}$ and $\overline{\{N_Q\}}$ have the same dimension and that it is equal to $\{q\}$ dimension. Then displacement can be described fields as:

$$u = \overline{\{N_P\}}^T \{q\} \text{ and } w = \overline{\{N_Q\}}^T \{q\} \quad (21)$$

The Lagrangian for free vibration is then written as:

$$L = T - U = \frac{1}{2} \left(\{\dot{q}\}^T [M] \{\dot{q}\} - \{q\}^T [K] \{q\} \right) \quad (22)$$

Minimizing the energy functional of Equation (22) the motion equation for undamped free vibration of thin curved beam elements becomes:

$$[M] \{\ddot{q}\} + [K] \{q\} = 0 \quad (23)$$

where, the elementary stiffness and mass matrices are written as:

$$[K]^e = \int_0^L \{z\}^T \begin{bmatrix} EA & 0 \\ 0 & EI \end{bmatrix} \{z\} \, ds \quad (24)$$

$$[M]^e = \int_0^L \rho A \begin{Bmatrix} \overline{N_P} \\ \overline{N_Q} \end{Bmatrix}^T \begin{Bmatrix} \overline{N_P} \\ \overline{N_Q} \end{Bmatrix} ds \quad (25)$$

with:

$$\{z\} = \begin{Bmatrix} \dfrac{d\overline{N_P}}{ds} + \dfrac{\overline{N_Q}}{R} \\ \dfrac{1}{R}\dfrac{d\overline{N_P}}{ds} - \dfrac{d^2\overline{N_Q}}{ds^2} \end{Bmatrix} \quad (26)$$

3.1 Hierarchical curved beam elements

The first hierarchical finite element proposed for curved beams uses the C^0 shape functions for describe the axial displacement (u) and the C^1 shape functions for describe the radial displacement (w). This element is called HFEM 1 and have 2 nodes and 3 nodal degrees of freedom $\left(u_i, w_i \text{ and } \dfrac{dw_i}{ds} \right)$ per node.

The second hierarchical finite element proposed for curved beams uses the C^1 shape functions for describe both the displacement fields. This element is called HFEM 2 and have 2 nodes and 4 nodal degrees of freedom $\left(u_i, w_i, \dfrac{du_i}{ds} \text{ and } \dfrac{dw_i}{ds} \right)$ per node. The two proposed HFEM are also described in Table 1.

Table 1. HFEM proposed elements

Element	Displacement	Shape Functions	Hierarchical p refinement
HFEM 1	u	C^0	Lobatto
	w	C^1	Bardell
HFEM 2	u	C^1	Bardell
	w	C^1	Bardell

4. NUMERICAL RESULTS

In order to evaluate the results obtained by the hierarchical finite elements proposed, some models are analyzed for their validation. The results are compared with analytical solution or other numerical solutions found in literature.

4.1 Ring's model

Given that the analytical solution for ring is available in literature [15] and taking advantage of the ring's symmetry one quarter of the ring is modeled, as shown in Figure 2.

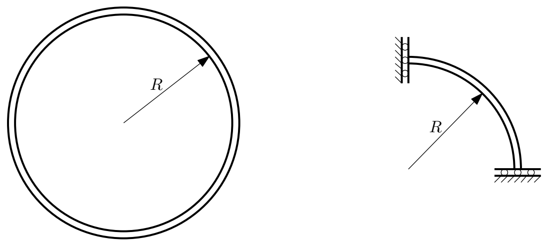

Fig. 2. Ring and one quarter of the ring scheme.

Given that only a quarter of the ring is modeled only the even frequencies of the full ring are obtained. The modeled ring has the following properties: cross-section 0.9525mm x 0.9525mm, radius of curvature of 0.3048m, material density of 1827.44 kg/m^3 and Young's modulus of 1.31×10^{11} N/m^2.

The first performed tests are convergence tests for the first frequencies of the ring. The results are compared with elements THIN^{01} and THIN^{11} [8] and the convergence tests are shown in Figures 3, 4, 5 and 6.

In order to evaluate the error the following expression was used:

$$\text{error} = \left| \frac{\omega_{appro} - \omega_{analy}}{\omega_{analy}} \right| 100\%, \quad (27)$$

where ω_{appro} is the frequency obtained numerically and ω_{analy} is the analytical frequency given by [15].

The convergence tests show that, mainly, for the first two frequencies the HFEM presents more accurate results in almost all the graphic area. For the last two frequencies, at the beginning of the graph the THIN^{01} and THIN^{11} elements present more accurate results, but at the end of the graph the HFEM presents more accurate results as well. Among the two proposed HFEM approaches, both have similar convergence rates.

The next presented result is the Mass matrix condition number also compared with THIN^{01} and THIN^{11} [8]. For the condition number, the lower its value the more numerically stable the system to be solved. The Mass matrix condition number is presented in Figure 7.

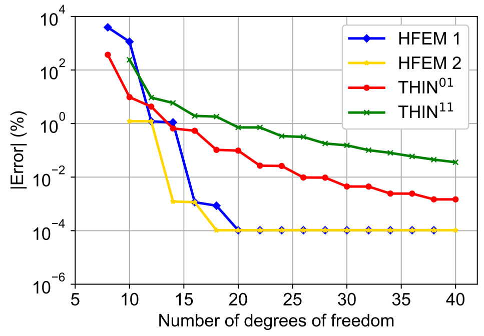

Fig. 3. Convergence of the second frequency of the ring.

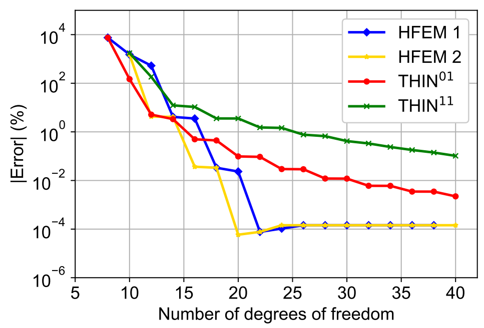

Fig. 4. Convergence of the fourth frequency of the ring.

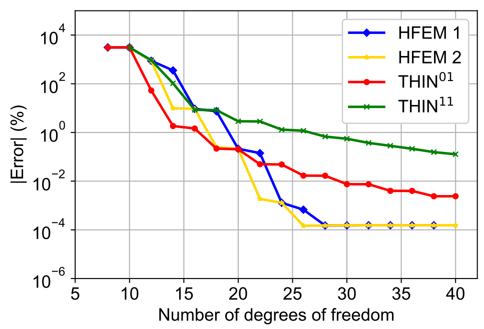

Fig. 5. Convergence of the sixth frequency of the ring.

Regarding the Mass matrix condition number, the THIN^{01} and THIN^{11} [8] elements present lower results and therefore are better compared to the proposed HFEMs. The proposed HFEMs condition numbers are quite similar, although HFEM 1 has slightly lower values.
Since the vibration modes are rarely found in the literature, the first three vibration modes obtained with HFEM 1 are presented in Figures 8, 9 and 10, which are very similar to those obtained with HFEM 2.

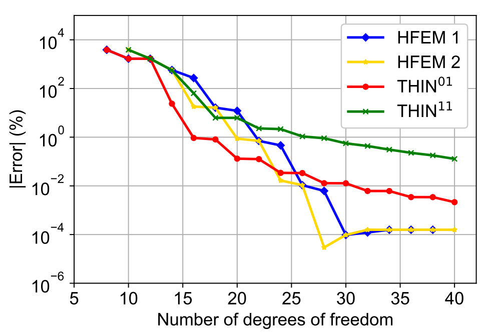

Fig. 6. Convergence of the eighth frequency of the ring.

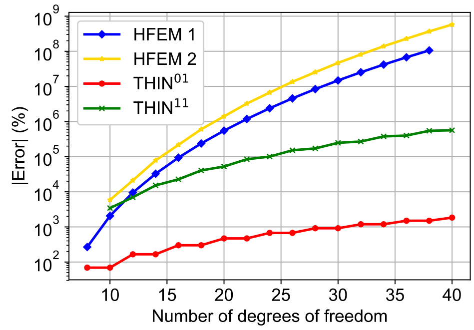

Fig. 7. Mass matrix condition number.

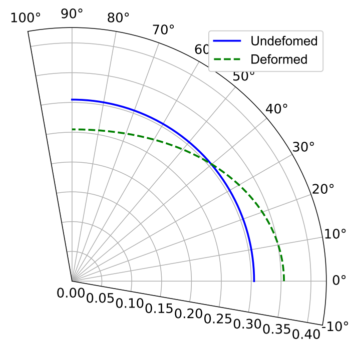

Fig. 8. Second vibration mode of the ring.

4.2 Pinned-pinned arch model

The second model analyzed is a pinned-pinned arch, as shown in Figure 11.
The arch is modeled with two configurations: the first one has the relation between radius of curvature (R) and gyration radious (r) of 25 and for the second one the relation is 140. The results are obtained as a function of the adimensional parameter (C_n) given by:

$$C_n = \omega_n \, L_e^2 \sqrt{\frac{\rho \, A}{E \, I}}, \tag{28}$$

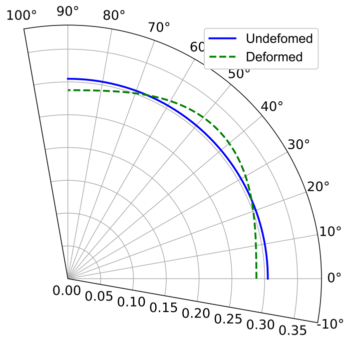

Fig. 9. Fourth vibration mode of the ring.

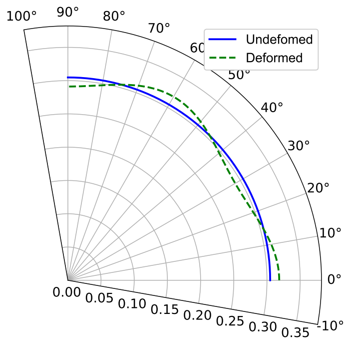

Fig. 10. Sixth vibration mode of the ring.

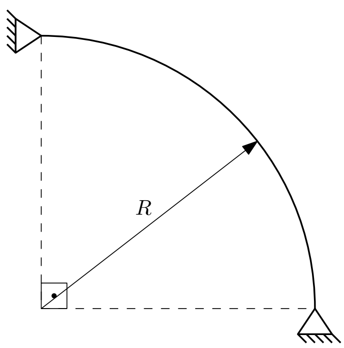

Fig. 11. Pinned-Pinned arch scheme.

where ω_n are the natural frequencies and L_e is the arch length.
The results of the proposed HFEM elements with 1 finite element are compared with the results found in [11] using the FEM with 8 finite elements with 4 nodal degrees of freedom and 1 non nodal degree of freedom, totalizing 44 degrees of freedom. The results are presented in Tables 2, 3, 4 and 5.
Firstly, the two proposed HFEMs present more accurate results than the reference solution even with a lower number of degrees of freedom for both arch configurations.

Table 2. Results of the six first parameters with $R/r = 25$ for HFEM 1.

Mode	HFEM 1			[11]
	14 d.o.f.	22 d.o.f.	30 d.o.f.	44 d.o.f.
1	33.95282	33.59056	33.59056	33.60
2	53.46808	53.41262	53.41262	53.42
3	90.12195	88.13527	88.13509	88.25
4	131.97712	129.94683	129.94226	130.72
5	174.91138	159.57218	159.52233	160.28
6	253.46729	236.71086	235.99315	239.16

Table 3. Results of the six first parameters with $R/r = 25$ for HFEM 2.

Mode	HFEM 2			[11]
	14 d.o.f.	22 d.o.f.	30 d.o.f.	44 d.o.f.
1	33.71414	33.59056	33.59056	33.60
2	53.46808	53.41262	53.41262	53.42
3	90.12195	88.13527	88.13509	88.25
4	134.33172	129.94683	129.94226	130.72
5	253.46729	159.57218	159.52234	160.28
6	269.43616	236.71086	235.99315	239.16

Table 4. Results of the six first parameters with $R/r = 140$ for HFEM 1.

Mode	HFEM 1			[11]
	14 d.o.f.	22 d.o.f.	30 d.o.f.	44 d.o.f.
1	37.06534	33.94930	33.94926	33.95
2	89.57846	79.62225	79.62141	79.73
3	315.30585	152.79327	152.06064	152.68
4	326.71114	235.28169	233.62636	235.77
5	569.55576	339.38050	337.70081	338.44
6	749.12055	387.25564	349.13637	355.52

Table 5. Results of the six first parameters with $R/r = 140$ for HFEM 2.

Mode	HFEM 2			[11]
	14 d.o.f.	22 d.o.f.	30 d.o.f.	44 d.o.f.
1	34.07940	33.94926	33.94926	33.95
2	89.57846	79.62225	79.62141	79.73
3	265.76061	152.25252	152.06060	152.68
4	326.71114	235.28169	233.62636	235.77
5	569.55576	339.38050	337.70081	338.44
6	767.41295	395.17663	349.13830	355.52

Comparing the results of HFEM 1 with HFEM 2, it can be observed that, in general, HFEM 1 presents more accurate results mainly for the higher frequencies.

5. CONCLUSION

In this paper two Hierarchical finite elements for thin curved beams were proposed, called HFEM 1 and HFEM 2.
Both the proposed elements presents more accurate results and better convergence rates compared with references solutions found in literature.
In Figure 7 the elements $THIN^{01}$ and $THIN^{11}$ presents better mass matrix condition numbers compared with HFEM 1 and HFEM 2, but the condition numbers of the proposed HFEM are not high enough to cause numerical instabilities.
Comparing HFEM 1 with HFEM 2 both have very similar convergence rates, but HFEM 1 seems to present more accurate results at higher frequencies.
Finally, the two finite hierarchical elements proposed are quite accurate and have good numerical stability.

6. REFERENCES

[1] N. M. Auciello and M. A. De Rosa. Free vibrations of circular arches: a review. *Journal of Sound and Vibration*, 4(176):433–458, 1994.

[2] N. S. Bardell. An engineering application of the h-p version of the finite element method to the static analysis of a euler-bernoulli beam. *Computers & Structures*, 59(2):195–211, 1996.

[3] S. D. Campion and J. L. Jarvis. An investigation of the implementation of the p-version finite element method. *Finite Elements in Analysis and Design*, 23:1–21, 1996.

[4] A. K. Chopra. *Dynamics of Structures: Theory and Applications to Earthquake Engineering*. Prentice Hall, New Jersey, 3 edition, 1995.

[5] D. J. Dawe. Numerical studies using circular arch finite elements. *Computers and Structures*, 4:729–740, 1974.

[6] A. Krishnan and Y. J. Suresh. A simple cubic linear element for static and free vibration analyses of curved beams. *Computers and Structures*, 68:473–489, 1998.

[7] A. W. Leissa and M. S. Qatu. *Vibrations of Continuous Systems*. McGraw-Hill, 2011.

[8] A. Y. T. Leung and B. Zhu. Fourier p-elements for curved beam vibrations. *Thin-Walled Structures*, 42:39–57, 2004.

[9] M. Petyt and C. C. Fleischer. Free vibration of a curved beam. *Journal of Sound and Vibration*, 18(1):1–30, 1971.

[10] R. Raveendranath, G. Singh, and B. Pradhan. A two-noded locking-free shear flexible curved beam element. *International Journal for Numerical Methods in Engineering*, 44:265–280, 1999.

[11] R. Raveendranath, G. Singh, and B. Pradhan. Free vibration of arches using a curved beam element based on a coupled polynomial displacement. *Computers and Structures*, 78:583–590, 2000.

[12] R. Raveendranath, G. Singh, and G. V. Rao. A three-noded shear-flexible curved beam element based on coupled displacement field interpolations. *Journal for Numerical Methods in Engineering*, 51:85–101, 2001.

[13] R. E. Rossi and P. A. A. Laura. Dynamic stiffening of an arch clamped at one end and free at the other. *Journal of Sound and Vibration*, 160:190–192, 1993.

[14] P. Solín, K. Segeth, and I. Dolezel. *Higher-Order Finite Element Methods*. CRC Press, 2004.

[15] S. Timoshenko. *Vibration Problems in engineering*. Van Nostrand, New York, 1955.

[16] F. Yang, R. Sedaghati, and E. Esmailzadeh. Free in-plane vibration of general curved beams using finite element method. *Journal of Sound and Vibration*, 318:850–867, 2008.